CDF Note 10355

Search for Anomalous Production of Photon + Jets + Missing Transverse Energy Events in $p\bar{p}$ collisions at $\sqrt{s} = 1.96$ TeV

The CDF Collaboration
URL http://www-cdf.fnal.gov
November 29, 2010

Abstract

Many new physics models predict mechanisms that could produce a γ+jets signature. We search in the γ+jets channel, independent of any model, for new physics using 4.8 fb^{-1} of CDF Run II data collected at the Fermilab Tevatron from $p\bar{p}$ collisions at $\sqrt{s} = 1.96$ TeV. A variety of techniques are applied to estimate the Standard Model expectation and non-collision backgrounds. We examine several kinematic distributions including photon E_T, invariant masses, and total transverse energy in the event for discrepancies with predictions of the Standard Model. We found data consistent with Standard Model expectation. This global search for new physics in γ+jets channel reveals no significant indication of physics beyond Standard Model.

1 INTRODUCTION

We present the preliminary findings of a model-independent, signature-based search for the anomalous production of γ + jets in $p\bar{p}$ collisions at $\sqrt{s} = 1.96$ TeV using 4.8 fb^{-1} of data recorded by the upgraded Collider Detector [1] at Fermilab (CDF II). We scan kinematic distributions including photon (γ) energy, invariant mass of the γ and leading jets, and total transverse energy in the event (H_T) for an excess of events over Standard Model (SM) predictions. An excess could indicate the existence of a new heavy particle decaying into γ + jets or a new physics mechanism such as gauge-mediated SUSY breaking [2] or Technicolor [3]. The Feynman diagrams in Fig. 1(a) and 1(b) illustrate examples of processes that yield the γ + 2 jets signature. Searching in the events with high $\not\!\!E_T$ may provide hints of SUSY like particles, $\tilde{\chi}_1^0 \to \gamma\tilde{G}$, with invisible decay.

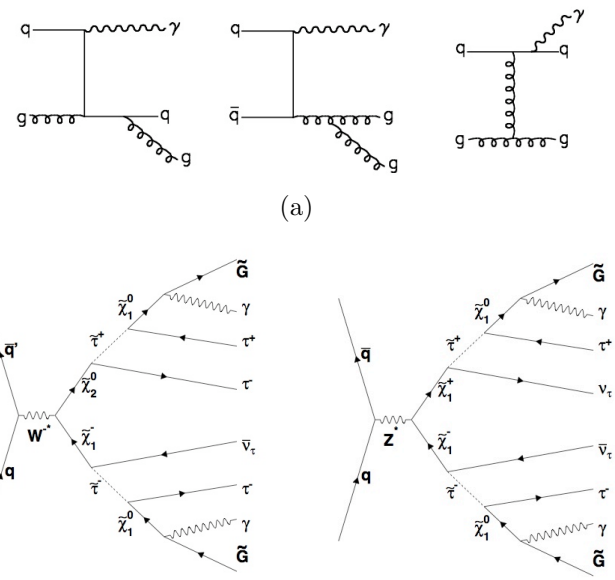

Figure 1: Feynman diagrams for tree-level (a) Standard Model and (b) GMSB processes that yield the γ + 2 jets signature.

2 DATA SAMPLE AND EVENT SELECTION

We select a sample of γ candidates by identifying isolated electromagnetic (EM) clusters with transverse energy $E_T > 30$ GeV in the central region of the calorimeter ($|\eta^{detector}| < 1.1$). In addition we require the EM cluster to pass standard photon candidate selection requirements [4]. To reduce the background from charged leptons, we require an absence of tracks pointing in the direction of the EM cluster. Background

from cosmic rays is reduced with a requirement on calorimeter EM timing [5], and we remove events that originate from the beam halo using a set of topological selection requirements that is orthogonal to photon selection [6]. Events with photomultiplier tube spikes — an instrumentation effect that can resemble a γ — are also removed. In the remaining event sample, we identify one or more jets with $E_T > 15$ GeV and $|\eta^{detector}| < 3.0$. The jet energy is corrected for detector response, energy loss, multiple $p\bar{p}$ interactions and underlying event [7]. Furthermore, an azimuthal separation of $\Delta\phi > 0.4$ radians between $\not\!\!E_T$ vector and any jet above $E_T > 15$ GeV is required to further reduce the effects of calorimeter energy measurement of the jets.

With above event selection, we select two data samples base on the number of jets with $E_T > 15$ GeV, $\gamma + \geq 1$ jet and $\gamma + \geq 2$ jet. Additional two subsamples with $\not\!\!E_T > 20$ GeV requirement is also chosen. By selecting events with significant $\not\!\!E_T$ the dominant SM γ and jet backgrounds are reduce and hence increasing our sensitivity to new physics which may produce large $\not\!\!E_T$. Each of the four data samples is compared with our background expectation.

3 MODELING BACKGROUNDS

The SM γ, SM diphoton, and SM charged lepton backgrounds are modeled using the simulated data from Pythia Monte Carlo generator (Tune A) [8]. All other backgrounds are modeled using data. Background from QCD multijet production, in which a jet fakes a photon, is modeled using a sample that consists of jets that pass looser photon selection requirements. Although a large portion of background from cosmic rays and the beam halo is removed by the γ + jets selection requirements, some events remain, and these backgrounds are significant in the large $\not\!\!E_T$ region. A pure cosmic ray event sample is attained using calorimeter EM timing information and is used to construct a background template. A set of topological cuts is used to select beam halo events. The beam halo and cosmic ray templates are normalized to the expected number of background events in the γ + jets sample. The SM diphoton and lepton templates are normalized according to the luminosity of the data. After subtracting all other backgrounds, the SM γ and multijet backgrounds are normalized according to the fake photon fraction which is determined to be $0.319 \pm 0.001(\text{stat}) \pm 0.0068(\text{syst})$ for photons with $E_T > 30$ GeV [9]. After proper normalization of each background, the number of data events will satisfy the following equation.

$$N^{data} = N^{SMphoton} + N^{qcd} + N^{diphoton} + N^{lepton} + N^{cosmic} + N^{beam\ halo} \tag{1}$$

where N is the total number of events in a given event sample. The distributions made using this formula or method will be referred to as *Method A*.

4 PRELIMINARY RESULTS

We present preliminary results in $\gamma + \geq 1$ jet and $\gamma + \geq 2$ jet event samples with and without the $\not\!\!E_T > 20$ GeV requirement. The Figures 2, 3, 4, and 5 show results without $\not\!\!E_T$ requirement. The Figures 6, 7, 8, and 9 show results with the $\not\!\!E_T$ requirement.

The data are represented by black dots and backgrounds are shown in different colors. The shaded region signifies the total systematic uncertainty. Uncertainty due to the jet energy measurement is by far the largest systematic uncertainty. Uncertainties on parton density functions (PDFs), initial and final state radiation (ISR/FSR), dependence on the renormalization, factorization and normalization scales (Q^2), uncertainty in the strong coupling constant (α_s), uncertainty in determining the fake photon fraction, integrated luminosity, EM energy measurements, beam halo estimate, and cosmic ray background estimate are also taken into account.

We have measured the photon E_T spectrum from 30 GeV to about 550 GeV, and over this range the total systematic uncertainty increases from 15% to 90%. It is evident that at higher E_T the photon purity increases. We are limited by statistics at high E_T. The invariant mass of the γ and the leading jet extends up to 1000 GeV. Many background predictions become limited by statistics in the high mass region, and the systematic uncertainty increases from 15% to 90%. As is evident from these plots, the SM γ and QCD multijet backgrounds are dominant. However with the requirement of large $\not\!\!E_T$ in the event, these backgrounds are reduced and the real $\not\!\!E_T$ from charged leptons decaying invisibly becomes significant. This $\not\!\!E_T$ requirement significantly improves the sensitivity to observing a heavy particle decaying invisibly. We see reasonable agreements between data and background in most of the distributions.

Figure 2: Kinematic distributions of $\gamma + \geq 1$ jet events using *Method A*

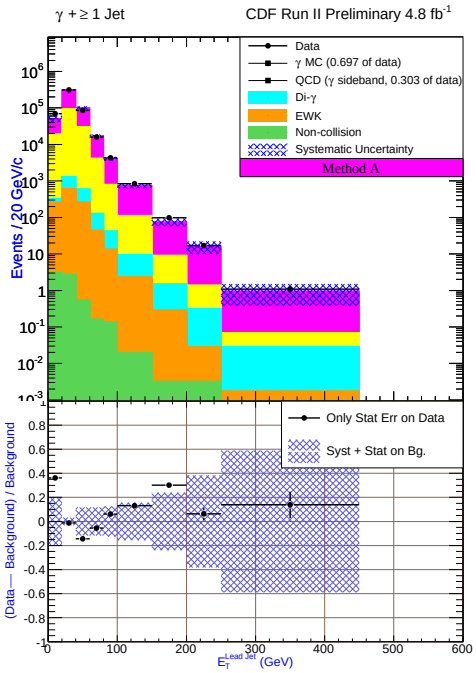

(a)

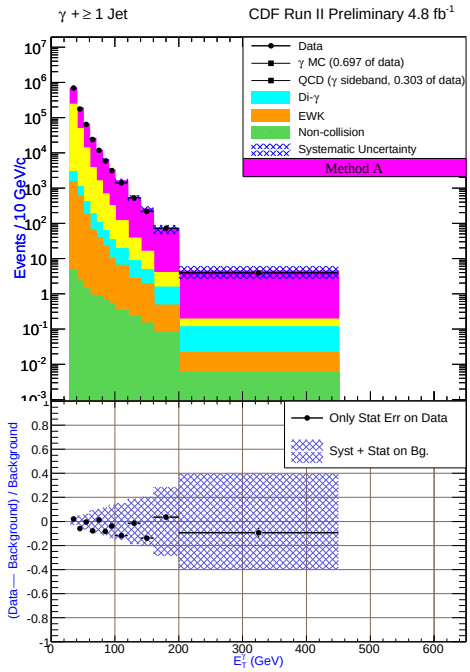

(b)

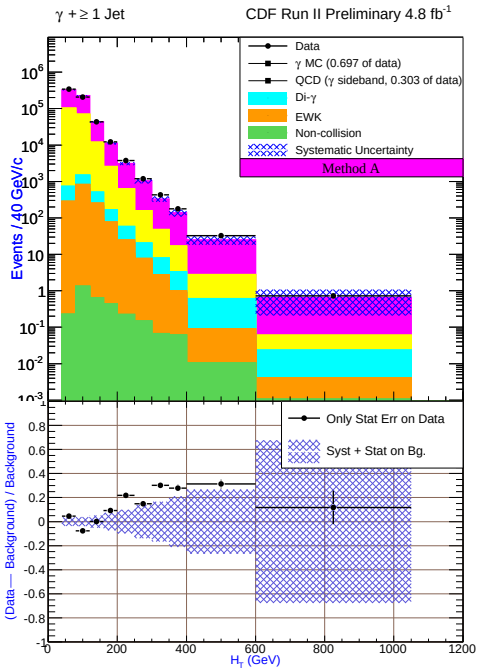

(c)

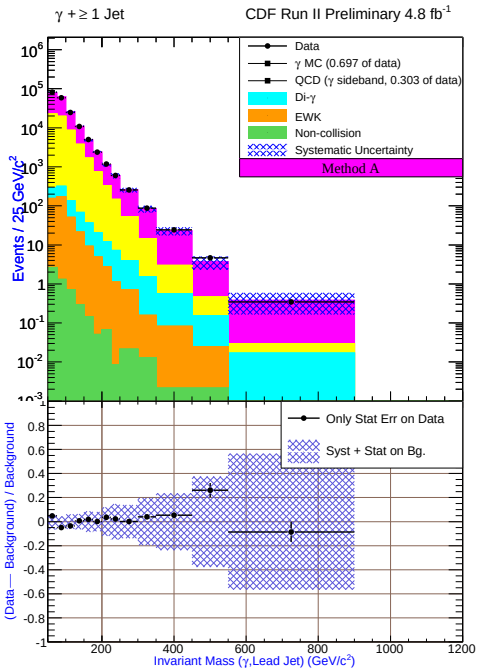

(d)

Figure 3: Kinematic distributions of $\gamma + \geq 1$ jet (top) and $\gamma + \geq 2$ jet (bottom) events using *Method A*

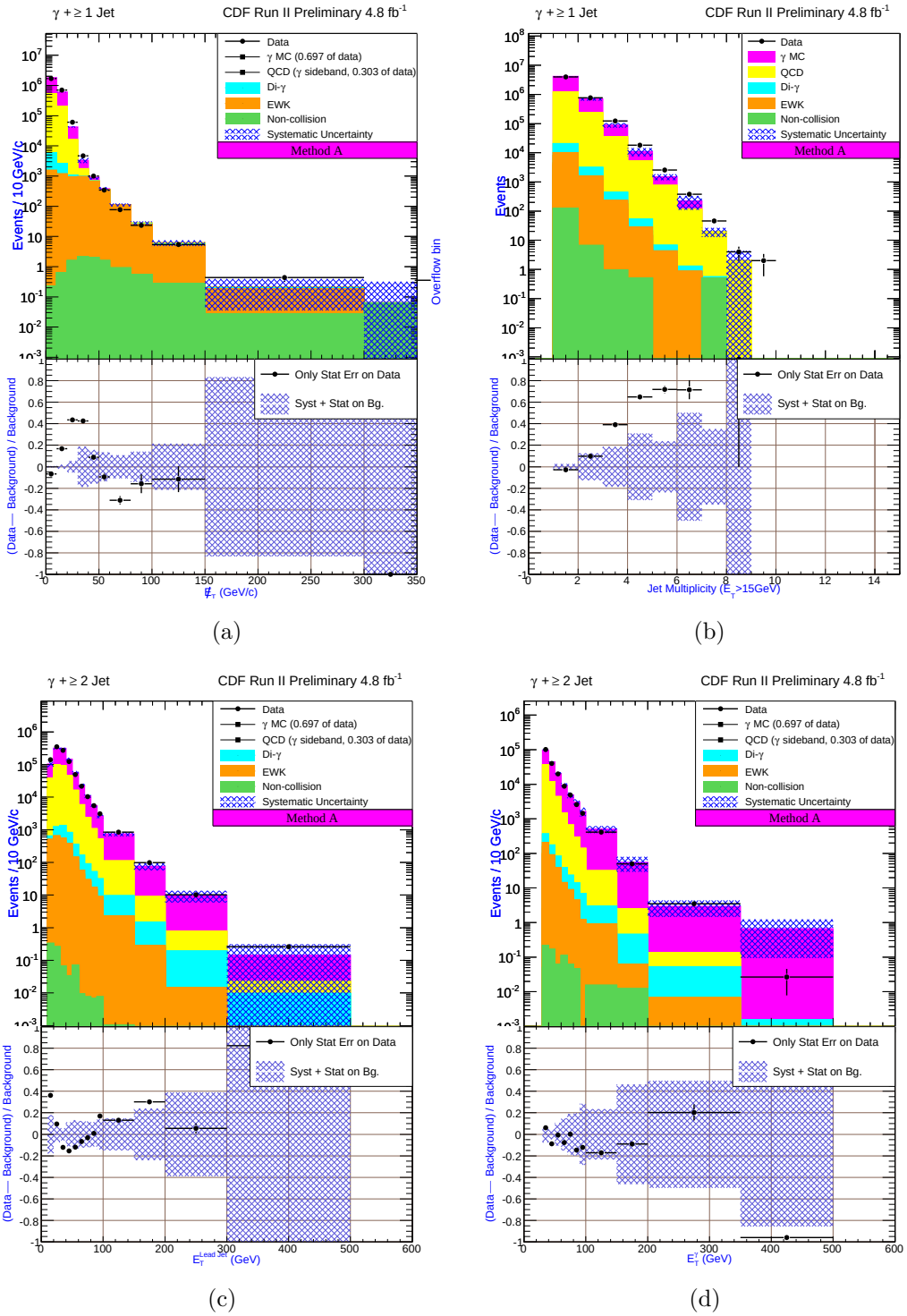

Figure 4: Kinematic distributions of $\gamma + \geq 2$ jet events using *Method A*

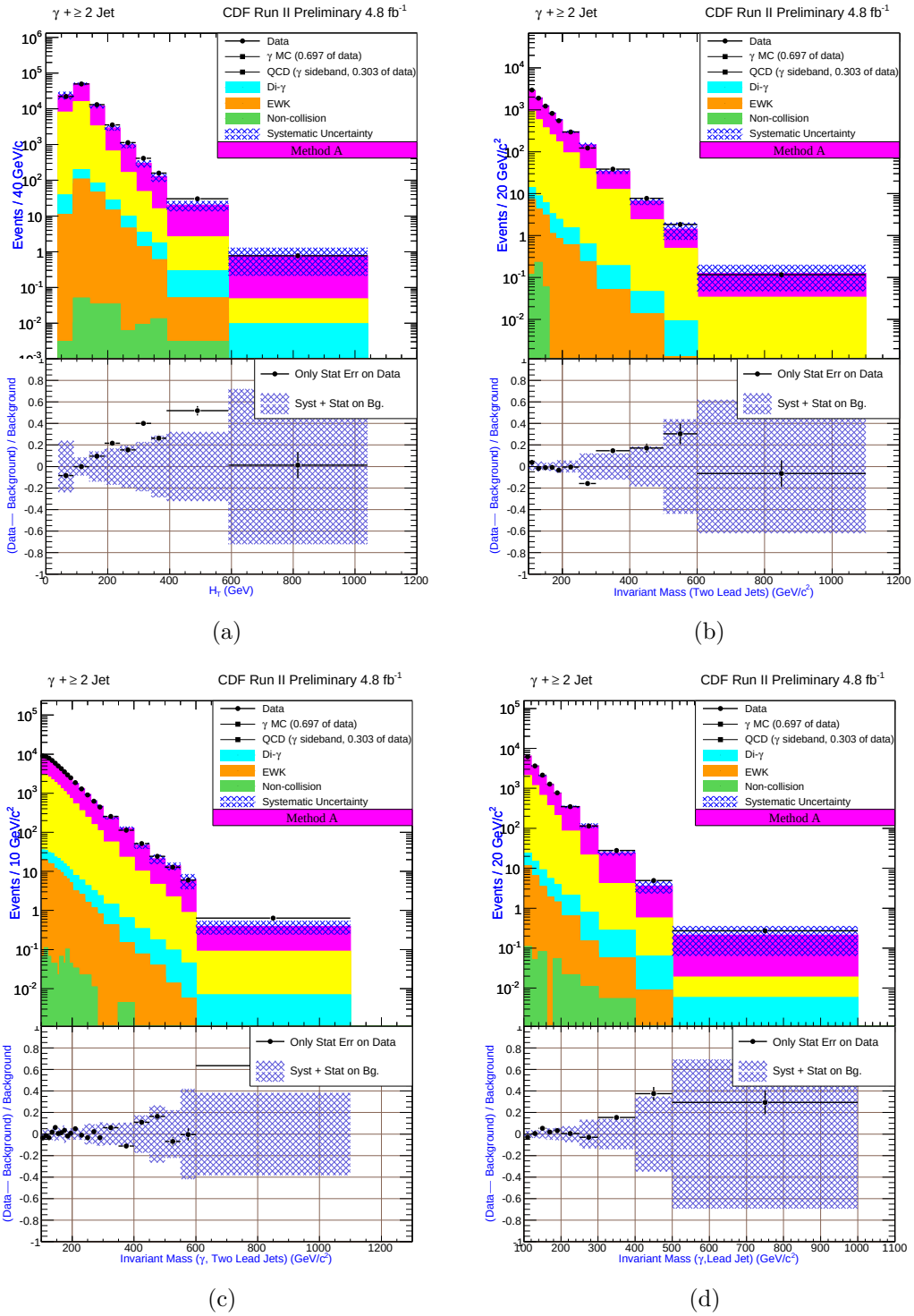

(a) (b) (c) (d)

Figure 5: Kinematic distributions of $\gamma + \geq 2$ jet events using *Method A*

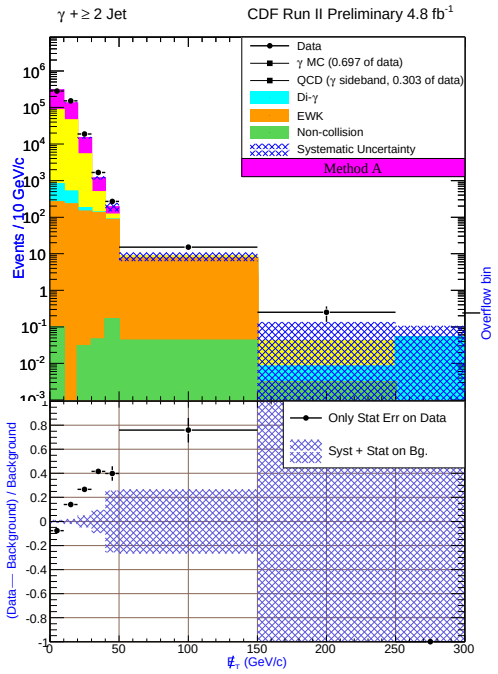

(a)

Figure 6: Kinematic distributions of γ + $\geq$1 jet + $\not\!\!E_T$ > 20 GeV events using *Method A*

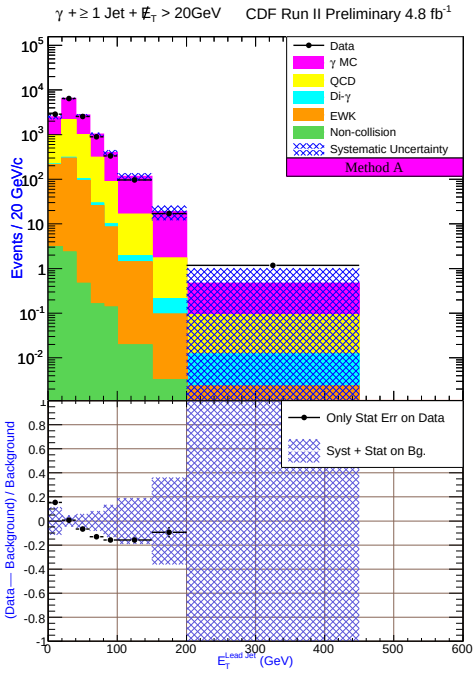

(a)

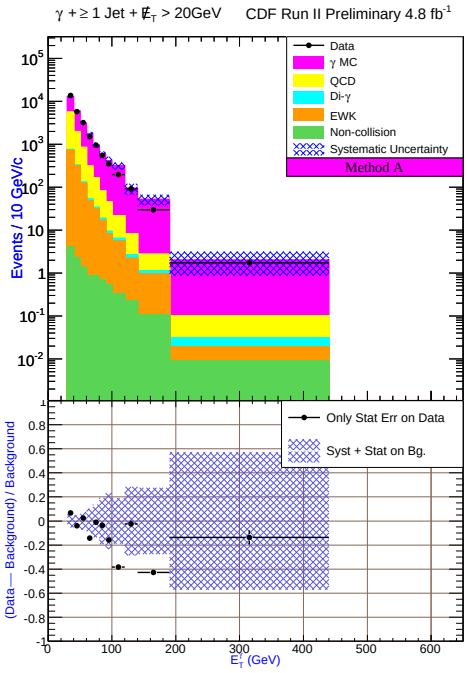

(b)

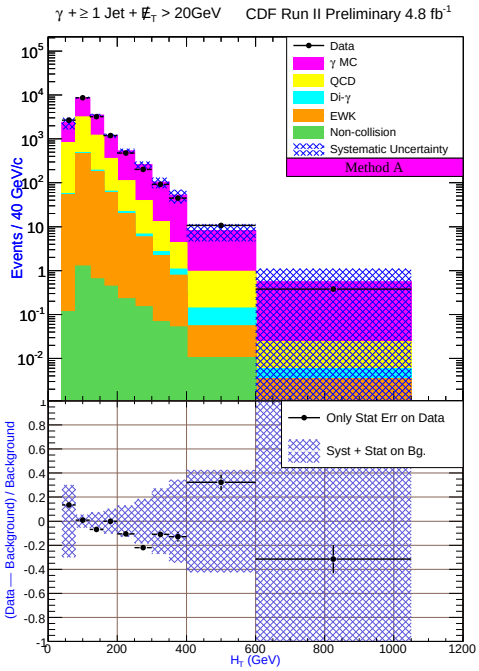

(c)

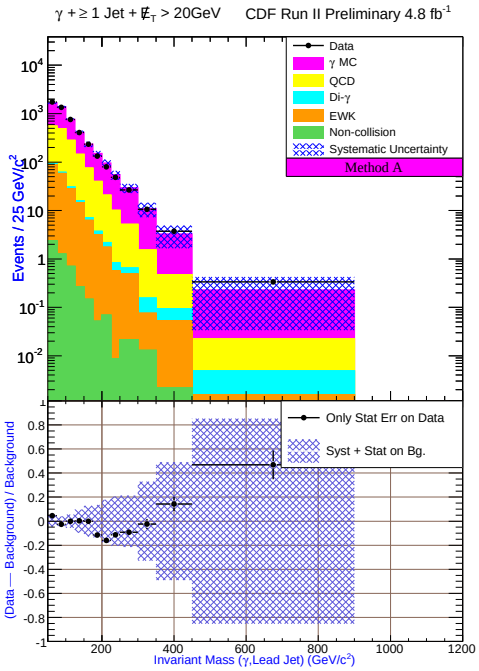

(d)

Figure 7: Kinematic distributions of γ + $\geq$1 jet +$\not\!\!E_T$ > 20 GeV (top) and γ + $\geq$2 jet +$\not\!\!E_T$ > 20 GeV (bottom) and events using *Method A*

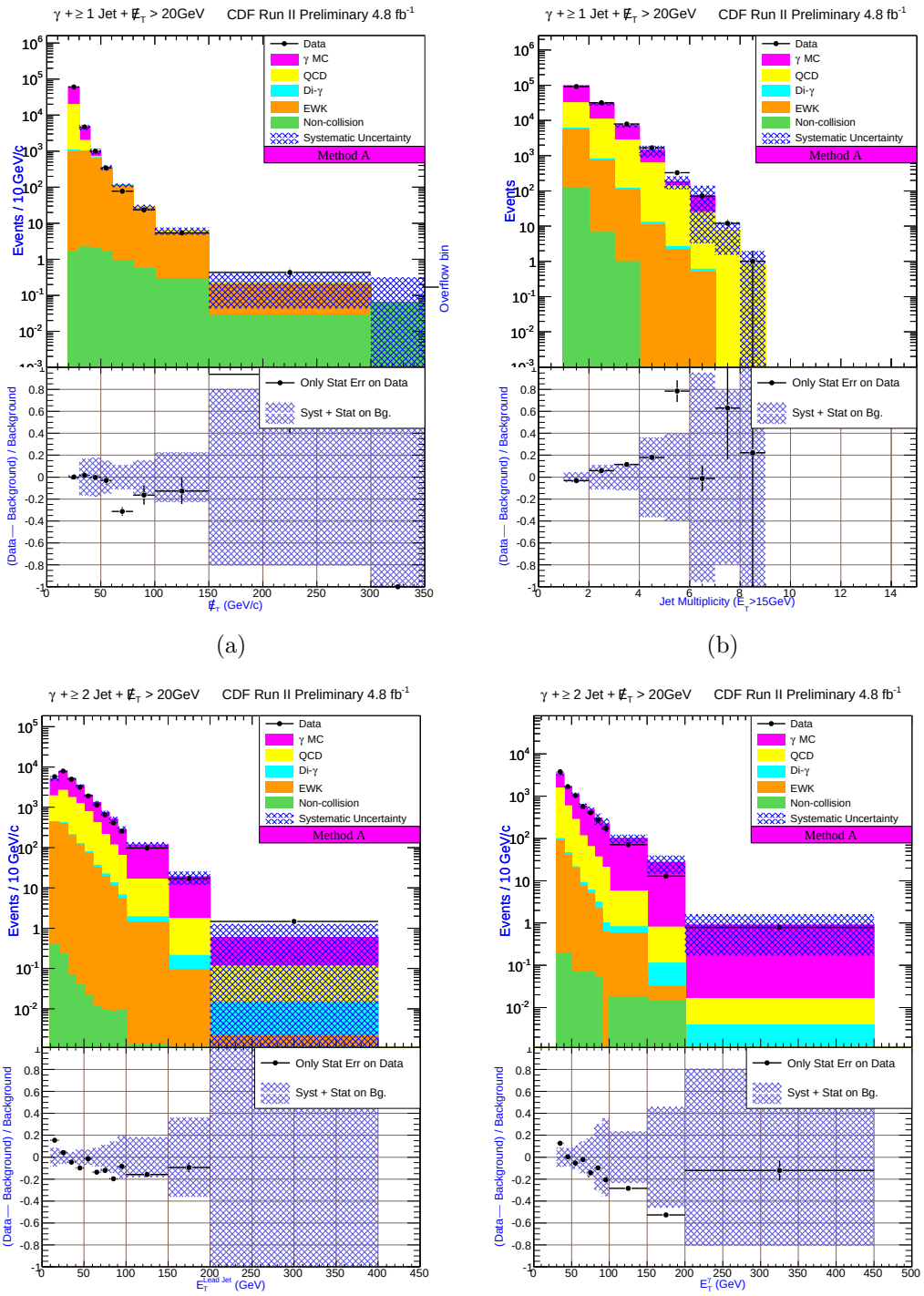

(a) (b)

(c) (d)

Figure 8: Kinematic distributions of γ + $\geq$2 jet + $\not\!\!E_T$ > 20 GeV events using *Method A*

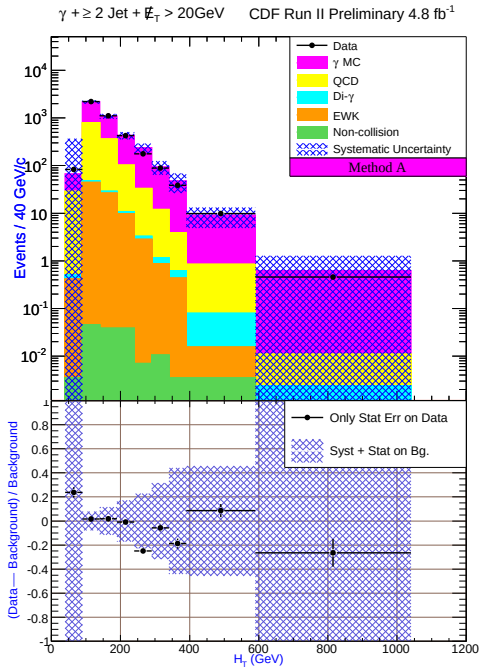

(a)

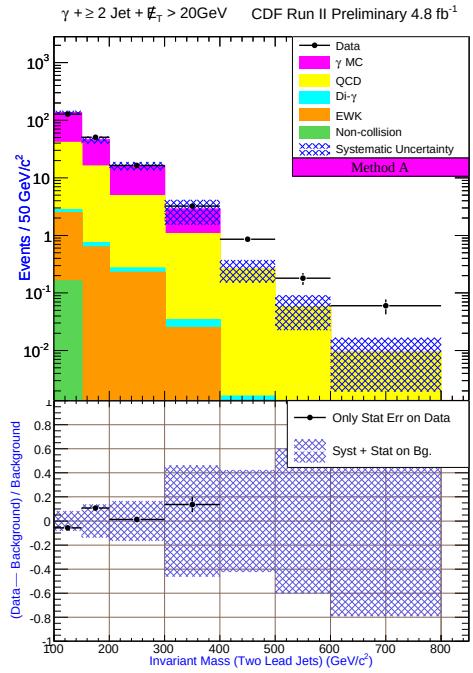

(b)

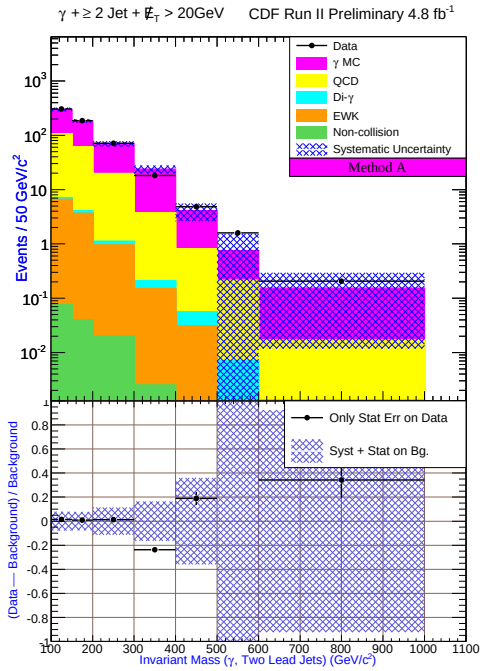

(c)

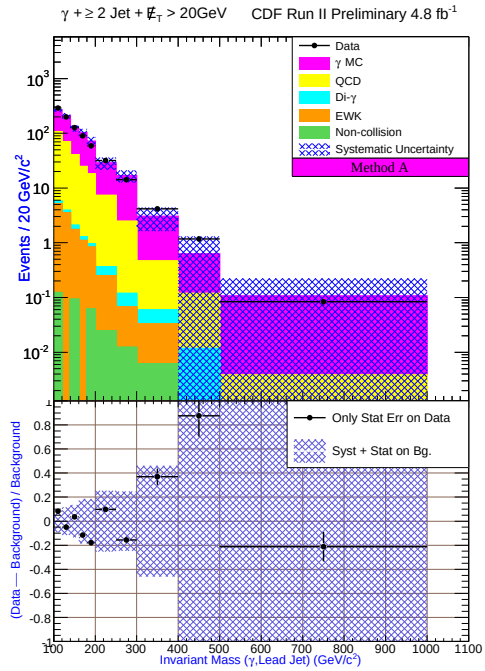

(d)

Figure 9: Kinematic distributions of γ + $\geq$2 jet +$\not\!\!E_T$ > 20 GeV events using *Method A*

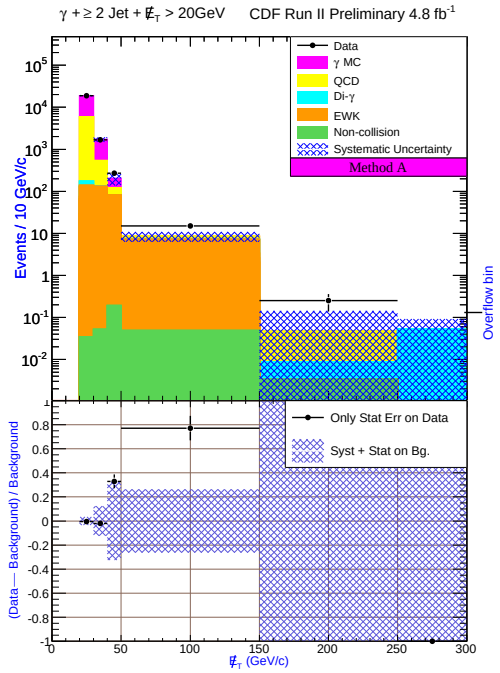

(a)

The backgrounds are well modeled and describes data reasonably well in most of the distributions. But a close inspection reveals certain distributions like, lead jet E_T, H_T, jet multiplicity and $\not\!\!E_T$, are discrepant and has certain structures. The deviations are not within the systematic uncertainty either. So we opted to further investigate and understand our background modeling in an attempt to understand the causes of such discrepancies.

It is a well known fact that Monte Carlo data has limitations in including next-to-leading order calculations. The PYTHIA events generator we have used to generate the Monte Carlo data samples includes only leading order Feynman diagrams. Hence all subleading jets are either from partons showering or from the overlaid minimum bias event. This directly affects the aforementioned kinematic variables. Furthermore, this causes the calorimeter $\not\!\!E_T$ resolution for Monte Carlo data to differ from collision data. Hence it is difficult to describe the low $\not\!\!E_T$ is region which is dominated by fake $\not\!\!E_T$ from jet energy mismeasurements using Monte Carlo data.

We developed a more data driven method in an attempt to understand and to overcome the limitations in the simulated data. In this method the control sample chosen to model the multijet (QCD) background is exploited as it is from real data. This sample of events is weighted in such a way that the E_T distribution of the QCD photon is matched to that of the combined QCD and SM photon E_T distribution using the fake photon fraction as shown in equation 2.

$$
\begin{aligned}
w &= \frac{\epsilon.MC}{(1-\epsilon)SB} \\
\Delta w &= w \pm (\frac{MC}{SB} - 1)\Delta\epsilon
\end{aligned} \tag{2}
$$

where

$$
\begin{aligned}
w &= \text{Weight for a given multijet bin} \\
MC &= \text{Photon Monte Carlo data events in that bin} \\
SB &= \text{multijet events in that bin} \\
\epsilon &= \text{True photon fraction} = 1.0 - \text{Fake photon fraction} \\
\Delta w &= \text{Propagated uncertainty of } w \\
\Delta\epsilon &= \text{Uncertainty of the true photon fraction}
\end{aligned}
$$

This *weighted* multijet event sample is used to model the distributions without the use of Monte Carlo data used to model SM photon fraction. We call this method, *Method B*. We have calculated an additional systematic uncertainty for reweighting procedure and is included in the *Method B* distributions. In *Method B*, the final event count can be summarized by equation 3 where N is the total number of events in a each event sample after proper normalization.

$$
N^{data} = N^{qcd\ weighted} + N^{diphoton} + N^{lepton} + N^{cosmic} + N^{beam\ halo} \tag{3}
$$

By using *Method B* we were able describe some distributions much better compared to *Method A*. Photon E_T distribution has to agree with *Method A* by construction and we cannot use it in the search. But the jet E_T, H_T, jet multiplicity and $\not\!\!E_T$ distributions show significant improvements and good agreements with data. The $\not\!\!E_T$ distribution agrees well in the low $\not\!\!E_T$ region. But some distributions were not modeled well as expected. For example the invariant mass of the photon and leading jet shows a large discrepancy which is attributed to the fact that the QCD sample is from different processes (or Feyman diagrams).

The Figures 10, 11, 12, and 13 show results without $\not\!\!E_T$ requirement. The Figures 14, 15, 16, and 17 show results with the $\not\!\!E_T$ requirement.

Figure 10: Kinematic distributions of $\gamma + \geq 1$ jet events using *Method B*.

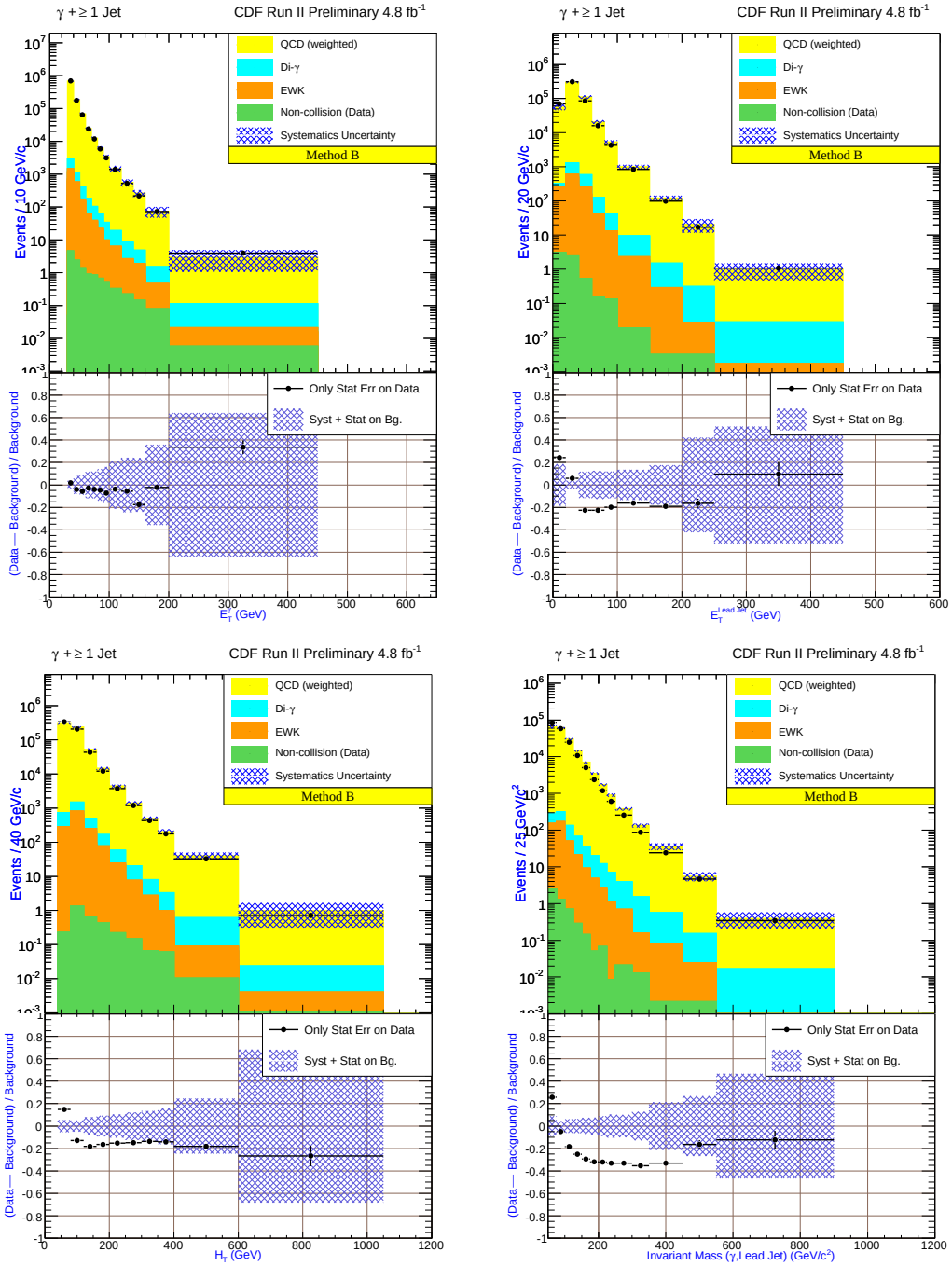

Figure 11: Kinematic distributions of $\gamma + \geq 1$ jet and $\gamma + \geq 2$ jet events using *Method B*.

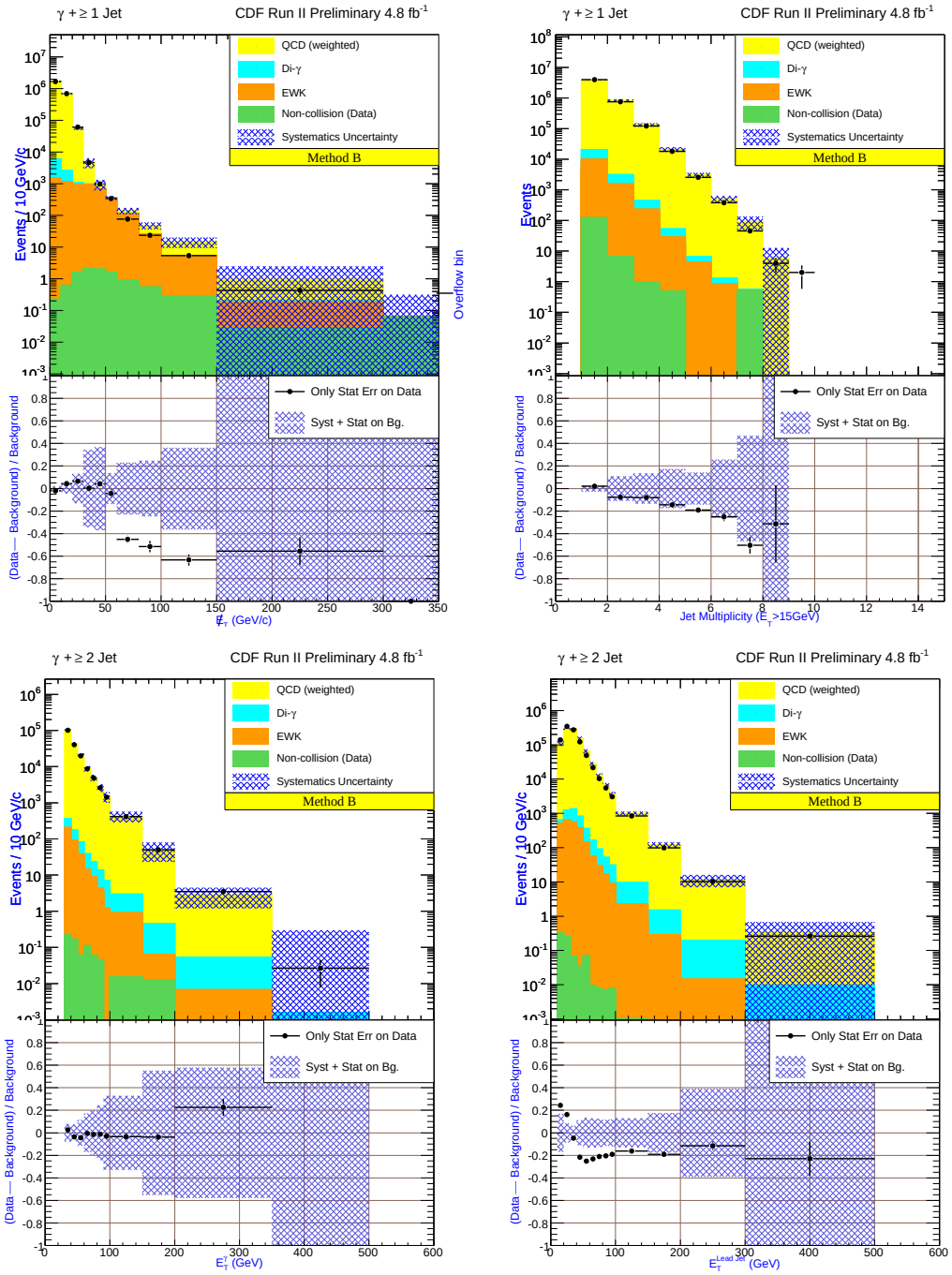

Figure 12: Kinematic distributions of $\gamma + \geq 2$ jet events using *Method B*.

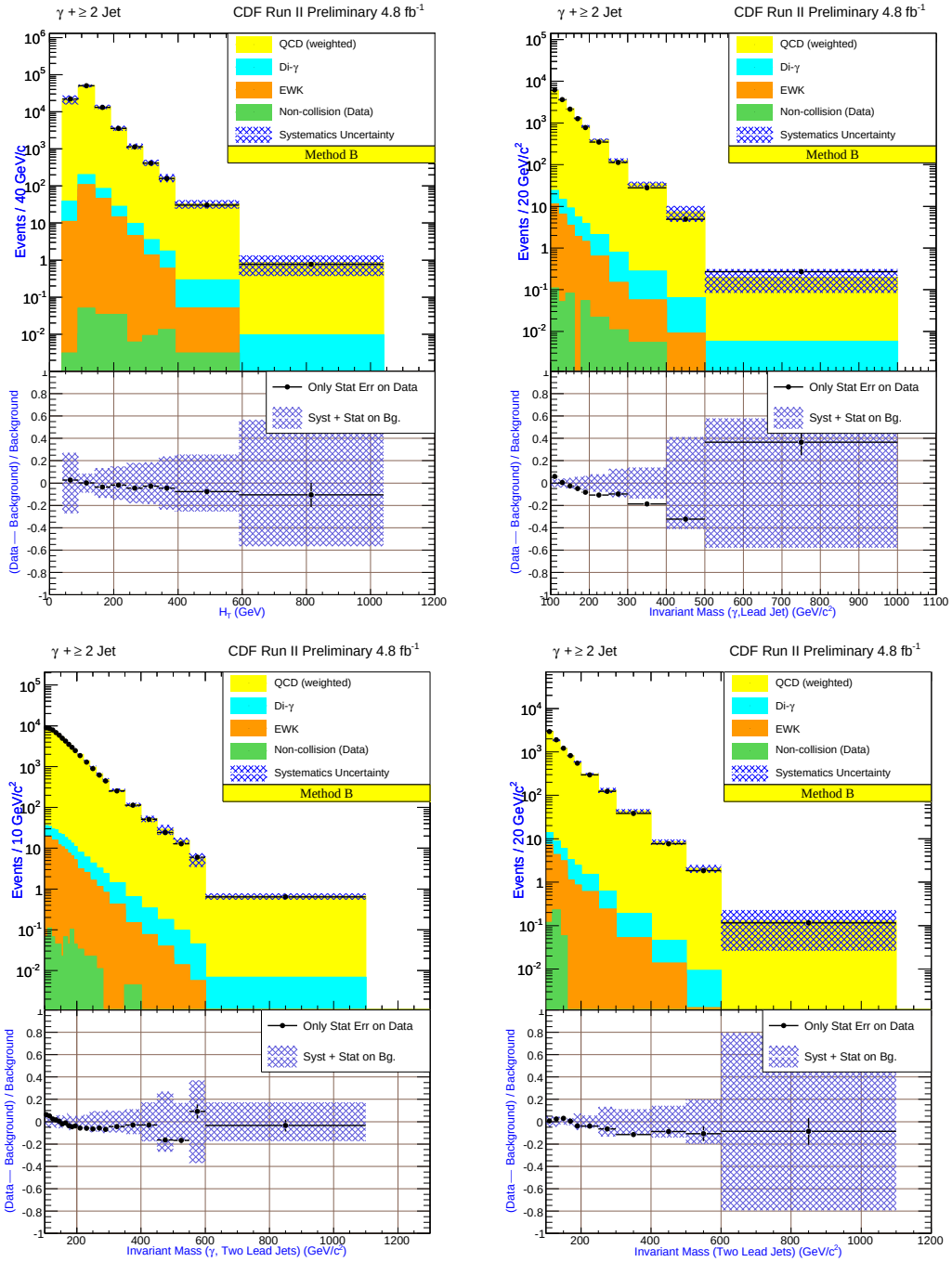

Figure 13: Kinematic distributions of $\gamma + \geq 2$ jet events using *Method B*.

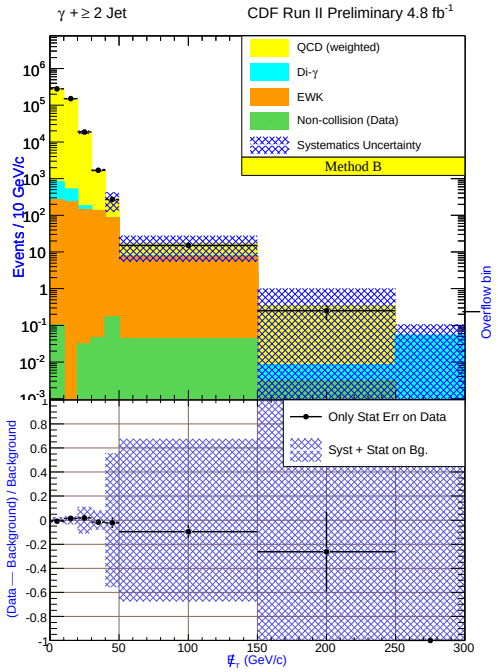

Figure 14: Kinematic distributions of $\gamma + \geq 1$ jet $+\not\!\!E_T > 20$ GeV events using *Method B*.

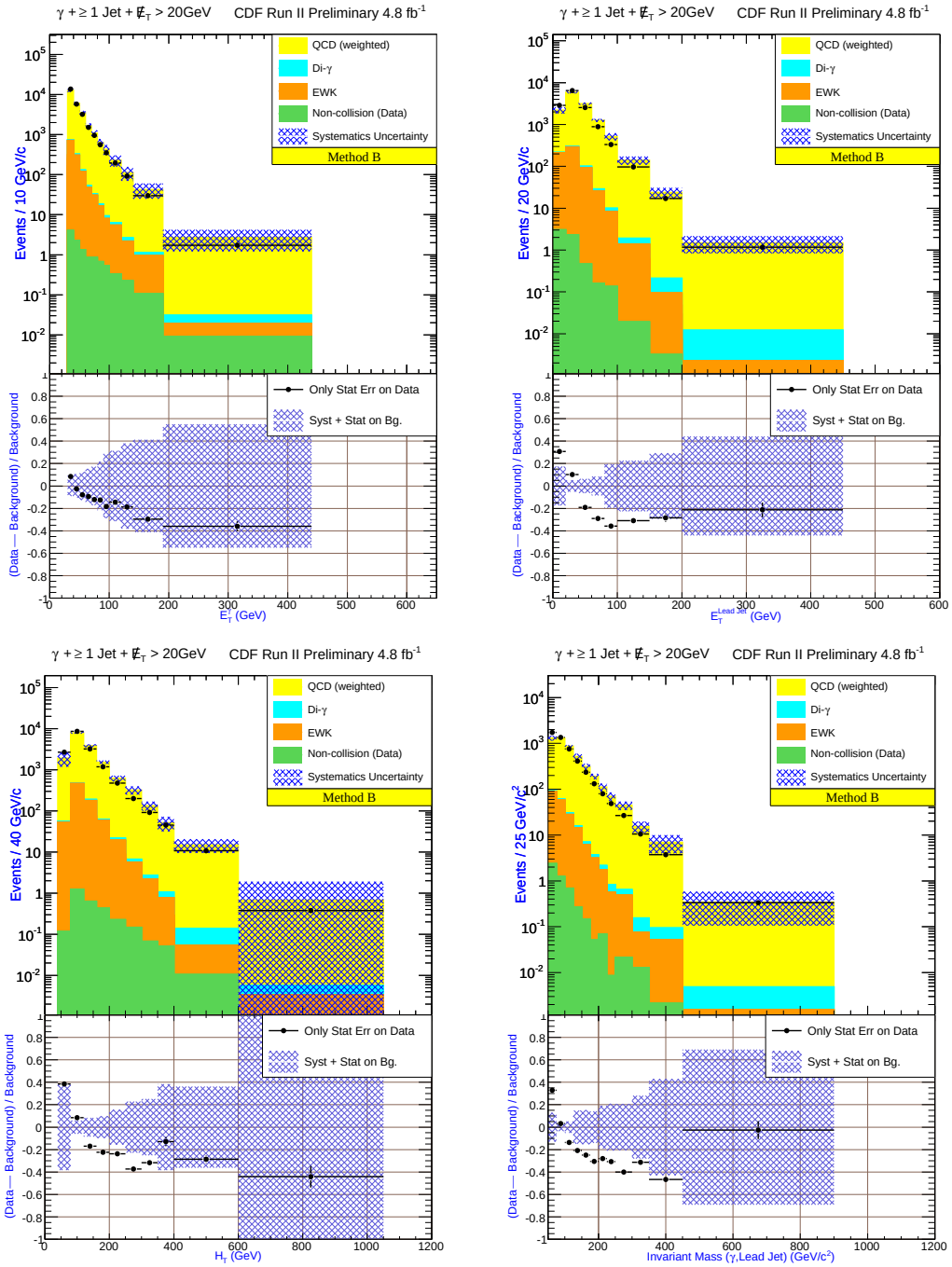

Figure 15: Kinematic distributions of γ + $\geq$1 jet +$\not\!\!E_T$ > 20 GeV and γ + $\geq$2 jet +$\not\!\!E_T$ > 20 GeV events using *Method B*.

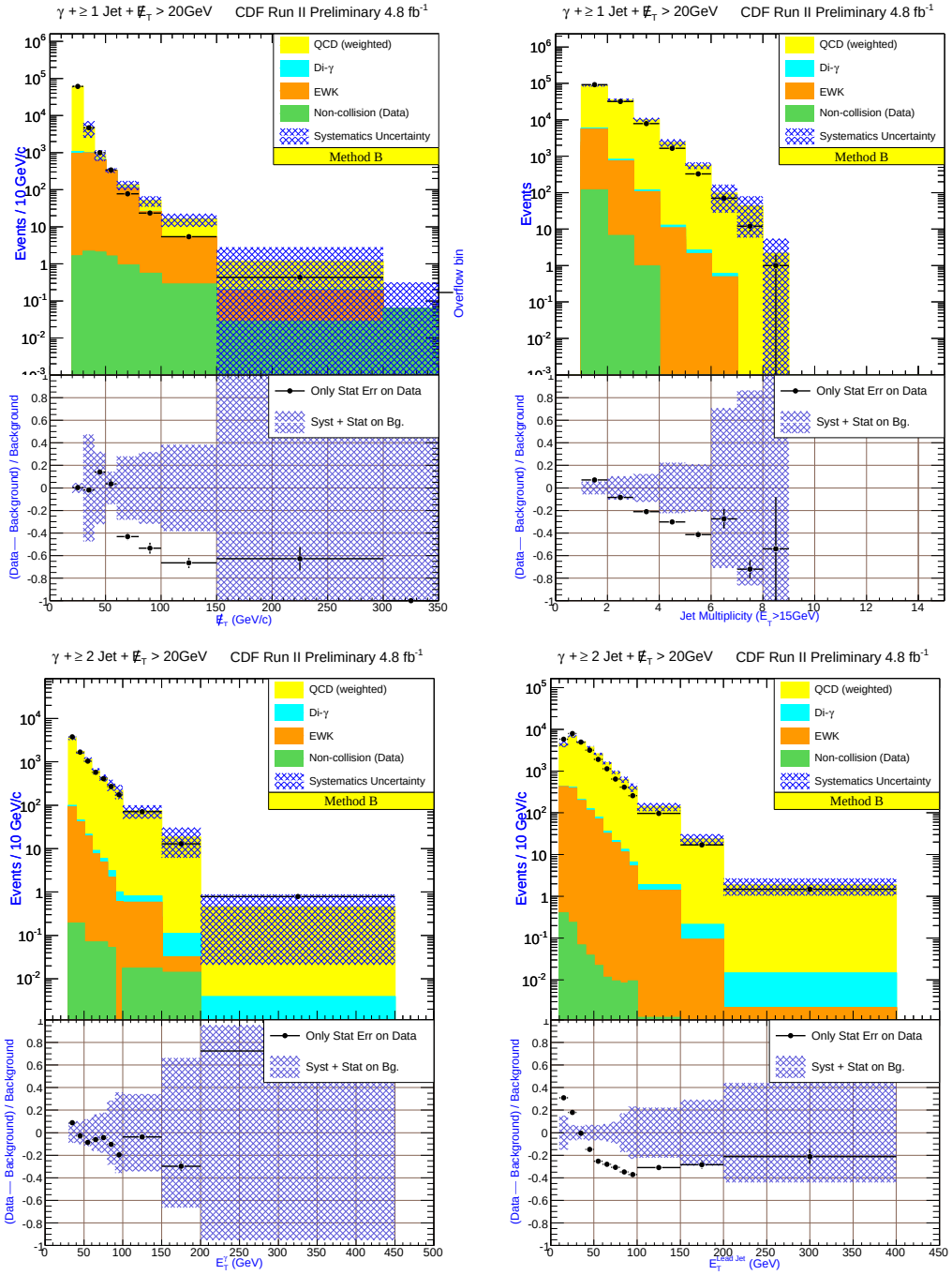

Figure 16: Kinematic distributions of $\gamma + \geq 2$ jet $+\not{E}_T > 20$ GeV events using *Method B*.

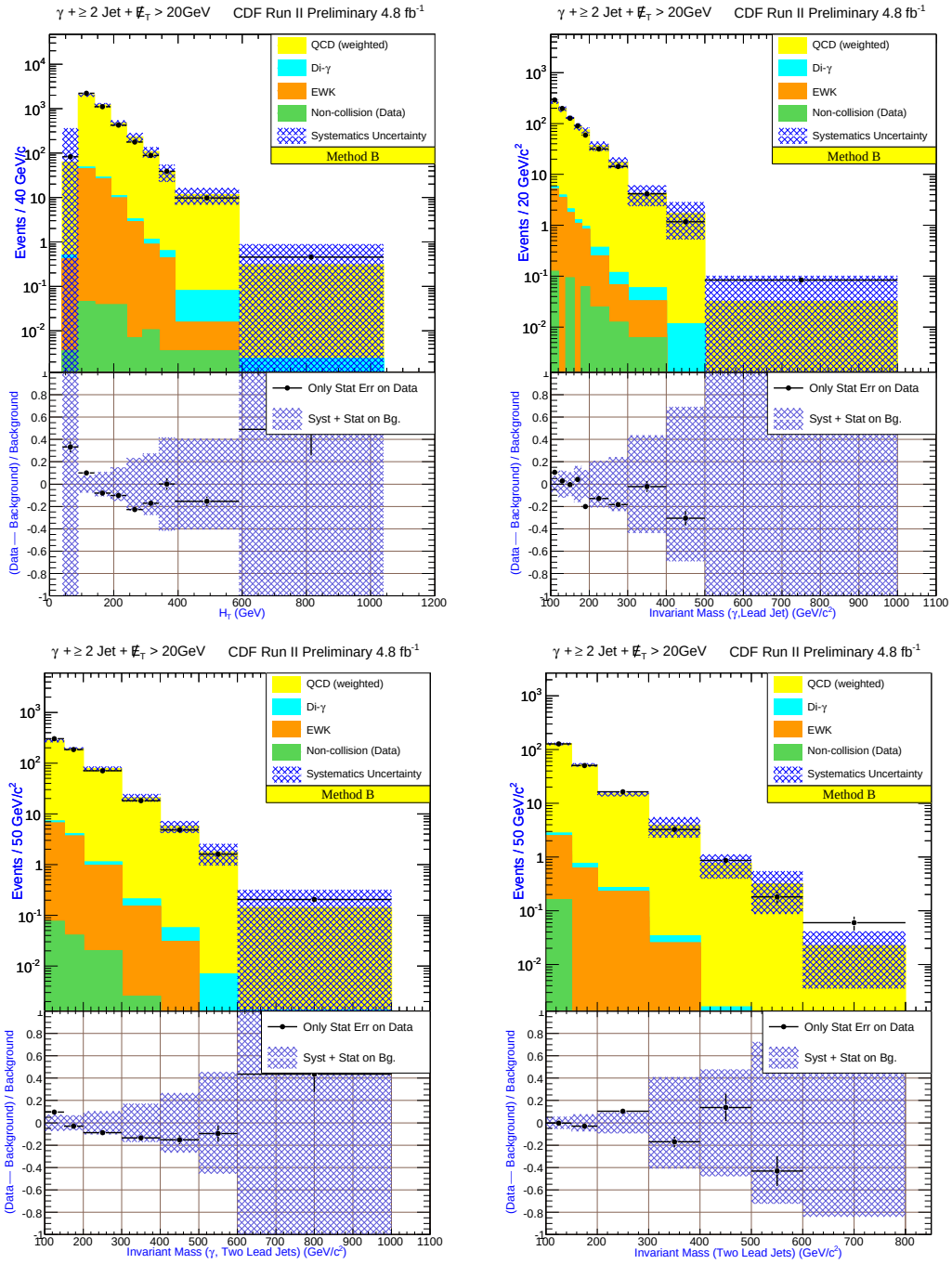

Figure 17: Kinematic distributions of $\gamma + \geq 2$ jet $+\not\!\!E_T > 20$ GeV events using *Method B*.

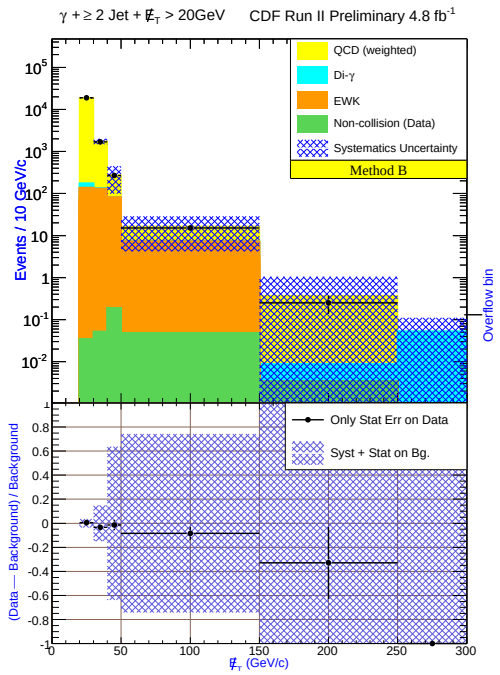

5 Conclusions

We have presented preliminary results of the search for beyond SM physics in $\gamma + \geq 1$ jet and $\gamma + \geq 2$ jet events with and without $\not\!\!E_T$ requirement. We have presented two different background prediction methods, *Method A* and *Method B*. Each method has proven to describe data with certain limitations. We think the two methods provide a greater understanding of data which otherwise may not be obvious and may have shown false results. Thus far, we see good agreement with the present theory predictions extending over several orders of magnitude. Search for new heavy particle in the high $\not\!\!E_T$ events has shown no significant deviation from data either. We conclude all our results are in agreements with the Standard Model expectation.

6 Acknowledgements

We thank the Fermilab staff and the technical staffs of the participating institutions for their vital contributions. This work was supported by the U.S. Department of Energy and National Science Foundation; the Italian Istituto Nazionale di Fisica Nucleare; the Ministry of Education, Culture, Sports, Science and Technology of Japan; the Natural Sciences and Engineering Research Council of Canada; the National Science Council of the Republic of China; the Swiss National Science Foundation; the A.P. Sloan

Foundation; the Bundesministerium für Bildung und Forschung, Germany; the World Class University Program, the National Research Foundation of Korea; the Science and Technology Facilities Council and the Royal Society, UK; the Institut National de Physique Nucleaire et Physique des Particules/CNRS; the Russian Foundation for Basic Research; the Ministerio de Ciencia e Innovación, and Programa Consolider-Ingenio 2010, Spain; the Slovak R&D Agency; and the Academy of Finland.

References

[1] F. Abe et al., Nucl. Instrum. Methods Phys. Res. A **271**, 387 (1988); D. Amidei et al., Nucl. Instum. Methods Phys. Res. A **350**, 73 (1994); F. Abe et al., Phys. Rev. D **52**, 4784 (1995); P. Azzi et al., Nucl. Instrum. Methods Phys. Res. A **360**, 137 (1995); The CDFII Detector Technical Design Report, Fermilab-Pub-96/390-E

[2] See for example S. Ambrosanio, G.L. Kane, G.D. Kribs, S.P. Martin, and S. Mrenna, Phys. Rev. D **54**, 5395 (1996); or C.-H. Chen and J.F. Gunion, Phys. Rev. D **58**, 075005 (1998).

[3] S. Weinberg, "Implications of Dynamical Symmetry Breaking: An Addendum" Phys. Rev. **D19** 1979 1277-1280.; L. Susskind, "Dynamics of Spontaneous Symmetry Breaking in the Weinberg-Salam Theory" Phys. Rev. **D20** strand, P. Ed n, C. Friberg, L.L (1979) 2619-2625.

[4] " http://www-cdf.fnal.gov/internal/physics/photon/docs/cuts.html"

[5] "The Timing System for the CDF Electromagnetic Calorimeters", Nucl.Instrum.Meth. A565:543-550,2006

[6] "Discrimination of Beam Halo and Cosmic Rays as a Source of Photon Candidates", M. Goncharov, V. Krutelyov, D. Toback, and P. Wagner, R. Culbertson, A. Pronko, CDF note 8409

[7] "Determination of the Jet Energy Scale at the Collider Detector at Fermilab", Nucl.Instrum.Meth.A566:375-412,2006

[8] T. Sjöstrand, P. Edén, C. Friberg, L. Lönnblad, G. Miu, S. Mrenna, and E. Norrbin, Comput. Phys. Commun. **135**, 238 (2001).

[9] Shin-Shan Eiko Yu, Ray Culbertson, "How to use CES and CPR Methods"; "http://www-cdf.fnal.gov/internal/physics/photon/docs/CesCprMethod.html"